Article

New insights into the enhancement effect of exogenous calcium on biochar stability during its aging in farmland soil

Hongyan Nan [1,2], Yunqiu Jiang [3], Weiqi Zhou [4], Ling Zhao [2,5] and Fan Yang [6,*]

[1] School of Chemical Engineering, Zhengzhou University, Henan 450001, China
[2] School of Environmental Science and Engineering, Shanghai Jiao Tong University, Shanghai 200240, China
[3] Hydrology and water resources Survey Bureau of the upper reaches of the Yangtze River, Hydrology Bureau of Yangtze River Water Resources Commission, Chongqing 400010, China
[4] Shanghai Investigation, Design & Research Institute Co., Ltd., Shanghai 200050, China
[5] China-UK Low Carbon College, Shanghai Jiao Tong University, Shanghai 201306, China
[6] School of Environment and Architecture, University of Shanghai for Science and Technology, Shanghai 200093, China
* Correspondence: yangfanusst@usst.edu.cn

Abstract: Converting biowaste into biochar and subsequently putting it into the soil are considered to be an effective approach to sequestrate carbon (C). However, biochar will inevitably undergo the aging process in soil, which influences its stability, and ultimately threatens its carbon sequestration ability. This study selected $CaCl_2$ as exogenous additive of sewage sludge and bone dreg to quantify both surface C and bulk C stability in Ca-rich biochars under three aging processes (dry-wet aging, freeze-thaw aging, and natural aging in farmland soil), and revealed the influence mechanisms of exogenous Ca on biochar stability. Results showed that after dry-wet aging (25 rounds), freeze-thaw aging (25 rounds), and natural aging in different farmland soils (5 months), oxidized surface C in Ca-rich biochar decreased by 10~23%, 28~41%, and 0~74%, respectively, compared to that in pristine biochar, while oxidized bulk C decreased by 6~10%, 0~1%, and 0~35%, respectively. Under three aging processes, the surface C and bulk C stability in Ca-rich biochar were superior to that in corresponding pristine biochar, which was attributed to the "protective effect" of Ca-containing crystals on biochar surface, including CaO, $Ca_5(PO_4)_3Cl$, $Ca_5(PO_4)_3(OH)$, $Ca_8H_2(PO_4)_6{\cdot}H_2O$ and $Ca_{10}(PO_4)_6(OH)_2$. These Ca-containing crystals could block the connection between biochar-C and the external oxidizing environment, intervening the oxidation of C-C/C = C in biochar, but also prevented aging from damaging C structure of biochar, reducing the generation of fragmented structure. By comprehensively assessing surface C and bulk C stability under three aging processes, final C sequestration in Ca-rich biochar increased to 27~80%, compared to that in pristine biochar (23~74%). Therefore, Ca-rich biochar is more dominant than pristine biochar, considering C sequestration potential during long-term aging in soil.

Keywords: Biochar aging; Ca-rich biochar; Carbon stability; Farmland soil; Carbon sequestration

1. Introduction

Following the 26th United Nations Climate Conference in 2021, the G20 Summit in 2022 proposes the goal of "the rise of global temperature being limited to 1.5 ℃" again, which requires the world to cut down 40% carbon emission by 2030. Biochar is a carbon-rich material generated from biowaste under O_2-limited and heating condition [1,2], and its application in soil can reduce CO_2 emission to the atmosphere during the global carbon cycle [3,4]. Biochar technology has been recognized as a promising approach to achieve long-term carbon sequestration [5]. However, due to the differences in feedstock and pyrolysis technology of biochar, some biochar can be retained in soil for thousands of years and others only for decades [6,7], which is closely related to biochar stability. Therefore, considering to improve biochar stability by regulating its formation during pyrolysis is of

 doi:10.20944/preprints202305.2235.v1

great significance for achieving carbon sequestration and emission reduction capacity of biochar.

Many previous studies have focused on the effects of feedstock type and pyrolysis conditions on biochar stability [8–12]. Feedstock compositions and contents are the decisive factor affecting biochar stability. The stability of biochar derived from ash-rich feedstock was higher than that derived from ash-poor feedstock, which should attribute to the encapsulation effect of ash on carbon [13]. Liu et al. [14] compared the stability of pig manure biochar with high ash content and rice straw biochar with low ash content, and found that the C stability in the former was higher than that in the later. Meanwhile, the difference of main carbon components in feedstock, including cellulose, hemicellulose, and lignin, also affect the stability of biochar. Higher lignin content in feedstock commonly led to a higher content of aromatic C in biochar and higher biochar stability [15]. Additionally, pyrolysis temperature has a significant role in determining the structure of biochar, thus influencing its stability. Usually, biochar produced at high temperature has stronger stability than that produced at low temperature, which attributes to that high temperature increases aromaticity and induces the formation of condensed graphitic structure in biochar [16]. For example, previous study reported that the unstable carbon in *Silphium perfoliatum L.* biochar decreased from 83.1% to 18.6% with increasing the pyrolysis temperature from 350 °C to 750 °C [17]. Chen et al. [18] also observed that with increasing pyrolysis temperature, the stability of biochar evaluated by $K_2Cr_2O_7$ was increased, and presented positive correlation with its aromatization degree. The above studies indicate that biochar stability can be improved by selecting some specific types of feedstock or by elevating the pyrolysis temperature of biochar. However, the selectivity of feedstock limits the universality of biochar, while high pyrolysis temperature increases energy consumption during producing biochar.

In recent years, many researchers found that adding exogenous minerals (K, Na, Ca, Mg, Fe, Al, P, Si, etc.) in feedstock before pyrolysis could improve C stability by changing the compositions and structure of biochar. On the one hand, these minerals could generate new crystals and wrap on the surface of carbon skeleton during pyrolysis, and they served as physical barriers to inhibit the oxidation of biochar. Our previous study has reported that by adding mineral K, Na, Ca, and Mg in biowaste, abundant mineral crystals, including KCl, NaCl, $CaCl_2$, $CaCO_3$, MgO and $MgO_3(CO_3)_2$, appeared on the surface of biochar. These crystals not only prevented the release of small molecules containing carbon during pyrolysis, but also prevented O_2 and microorganisms from entering the interior of biochar, thus enhancing the thermal oxidation resistance and microbial oxidation resistance of biochar [19]. On the other hand, some minerals have also been shown to bond with carbon or carbon-containing groups to form new compounds during pyrolysis, thus increasing the energy required for carbon degradation. For instance, Rosas et al. and Wu & Radovic [20,21] found that H_3PO_4 could combine with carbon to form a substance similar to C-O-PO_3 or $(CO)_2PO_2$ during pyrolysis, which was wrapped on the surface of carbon skeleton and strengthened the oxidation resistance of solid biochar products. Additionally, some minerals could form organometallic complexes with carbon. For example, mineral Si in biowaste interacts with C to generate organometallic C-Si couplings during pyrolysis [22,23], while mineral Fe can generate Fe-O-C organometallic complexes [24], and they are beneficial to improve the stability of biochar. However, until now, most of these studies focused on the effect of exogenous minerals on biochar stability during pyrolysis, while there is a lack of post assessment about the influence of exogenous minerals on biochar stability under long-term aging, and even rare research has revealed the underlying mechanisms.

Calcium (Ca), as a ubiquitous mineral in soil, is an environmentally friendly additive with low price. Therefore, in this study, $CaCl_2$ was used as exogenous calcium to prepare Ca-rich biochar using two biowastes, sewage sludge and bone dreg, and the effects of exogenous calcium addition on C stability in biochar were investigated by three aging methods: dry-wet alternating, freeze-thaw cycles, and natural farmland soil incubation. A se-

 doi:10.20944/preprints202305.2235.v1

ries of experiments were conducted: (1) to investigate the influence mechanism of exogenous Ca on surface C stability in biochar under the above three aging methods; (2) to reveal the influence mechanism of exogenous Ca on bulk C stability in biochar under the above three aging methods; and (3) to evaluate the enhancement effect of exogenous Ca on overall biochar stability based on the results of surface C and bulk C.

2. Materials and Methods

2.1. Preparation and characterization of pristine biochar and Ca-rich biochar

Sewage sludge (SS) and bone dreg (BD) were selected as the feedstock for producing biochar. SS was collected from the sewage treatment plant, Minhang, Shanghai. BD was purchased from a farmers' market in Shanghai. The two biowastes were dried at 60 ℃ in the oven for 24 h. Introducing calcium (Ca) in SS and BD was used to produce Ca-rich biochar. Specifically, 20 g $CaCl_2$ was dissolved in 1.5 L deionized water to prepare a solution, which was then mixed with 50 g biowaste (SS or BD). The mixture was stirred and dried in an oven at 60 °C to remove the whole water. Then two biowastes and corresponding Ca-rich biowastes were grinded to small grains with particle size less than 2 mm. The grinded biowaste was subjected to the pyrolysis process under N_2 atmosphere with a heating rate of 10 °C·min^{-1} and hold at the highest treatment temperature 500 °C for 2 h. The obtained biochar was grinded and passed through 0.5 mm size for later experiments. The two pristine biochar and corresponding Ca-rich biochar samples were labelled as SSBC, BDBC, Ca-SSBC, and Ca-BDBC, respectively. The basic physicochemical characteristics of all biochar were shown in Table S1.

The elemental C, N, H, and O contents of biochars were determined using an elemental analyzer (Vario Macro Cube, German Elemental Analysis Systems Inc, Germany). The morphological and structural characterization by scanning electron microscope (SEM) (D/max-2200/PC, Japan Rigaku Corporation). The surface functional groups on biochar were identified by X-ray photoelectron spectroscopy (XPS) (AXIS Ultra DLD, Shimadzu Kratos, Japan). Surface crystalline compositions of biochar were collected using an X-ray diffractometer (XRD) D/max-2200/PC, Rigaku, Japan).

2.2. Experiments to simulate the dry-wet and freeze-thaw aging processes of biochar

Dry-wet aging and freeze-thaw aging are two common methods to simulate the aging of biochar in real environments [25,26]. All aging experiments were implemented in glass petri dishes (10 cm inner diameter) filled with fresh biochar. Then deionized water was added to make the maximum water holding capacity of the biochar reach 100%. Both dry-wet and freeze-thaw aging processes of biochar undergo with 25 rounds. Specifically, for each dry-wet cycle, the samples were incubated at 25 °C for 12 h and then dried at 60 °C in an oven for another 12 h. For each freeze-thaw cycle, the samples were incubated at 25 °C for 12 h and then frozen at −20 ℃ for another 12 h. Each cycle was repeated 25 times in total, and samples were collected after 5, 10, 15, and 25 cycles. All samples were frozen-dried and then grounded through a 2-mm sieve for the further characterization.

2.3. Measure of carbon stability in biochar

Surface C stability. The surface C stability in biochar was calculated by contrasting the carbon content in biochar before and after aging (eq.1). In the formula, C_{before} and C_{after} are the C contents (%) in biochar before and after aging, respectively.

$$\text{Oxidized surface C (\%)} = \frac{C_{before} - C_{after}}{C_{before}} \times 100\% \quad (1)$$

Bulk C stability. The bulk C stability in biochar could be assessed via chemical $K_2Cr_2O_7$ oxidation, which could simulate the disintegration of carbon skeleton in a simulative extreme oxidation environment. Specifically, 0.1 g C of biochar was treated in a glass test tube with 40 mL of 0.1 M $K_2Cr_2O_7$ + 2 M H_2SO_4 solution at 55 ℃ for 60 h. Results were expressed as the fraction of total C oxidized by $K_2Cr_2O_7$.

 doi:10.20944/preprints202305.2235.v1

2.4. Experiments to simulate the natural aging process of biochar in different farmland soils

Based on geographical distribution, three typical farmland soils were selected for exploring the differences of carbon stability with applying pristine biochar and Ca-rich biochar in soil, including red soil in Hainan, yellow soil in Shaanxi, and paddy soil in Changshu. All farmland soil samples were sampled at a depth of 0~20 cm on the soil surface, air-dried and ground, and then passed through a 2 mm sieve. The basic physical and chemical properties of three farmland soils are shown in Table 1.

Table 1. Selected properties of different farmland soils.

Farmland soil	pH	Sand %	Silt %	Clay %	K g·kg^{-1}	Na g·kg^{-1}	Ca g·kg^{-1}	Mg g·kg^{-1}	Fe g·kg^{-1}	Al g·kg^{-1}
Red soil	4.90	46.8	29.9	23.3	6.2	0.82	0.93	0.60	62.0	57.1
Yellow soil	9.10	21.3	69.8	8.97	12.1	1.02	31.7	5.83	13.0	13.4
Paddy soil	6.27	6.34	79.2	14.4	25.2	1.76	4.73	5.05	19.6	27.3

The co-culture experiment of biochar and farmland soil was performed in the container that was shaded around. Fifteen treatments were set, including three farmland soils (red soil, yellow soil, and paddy soil) and three farmland soils with the addition of four biochar samples (biochar: soil = 10% (*w*/*w*)). All treatments were conducted in triplicates. The water content of each treatment was kept as 70% water holding capacity. After 5-month experiments at room temperature, all treatments were dried and passed through a 2-mm sieve for further characterization. The evaluation methods of surface C and bulk C stability were as above Section 2.3.

2.5. Statistical analysis and quality control

All experimental data were set up in three parallel tests. The collected data were analyzed using Origin 2022b software. The statistical analyses were conducted using SPSS 24.0 at the 0.05 probability level, and all experimental data were presented as mean values ± standard deviations (n = 3).

3. Results and discussion

3.1. Exogenous calcium served as an "armor" to protect C during biochar aging

Change of main elements. Figures 1 and S1 showed the evolution of C, O, H, and N elements in biochar under dry-wet and freeze-thaw aging processes. The C contents in SSBC and BDBC were 24.2% and 17.2% (Figures 1a and 1c), and they decreased continuously with the increase of aging rounds. Ultimately, after 25 dry-wet and freeze-thaw aging rounds, C contents in SSBC decreased by 21.9% and 17.0%, respectively, and that in BDBC decreased by 34.7% and 29.0%, respectively. The C loss was attributed to the oxidation and decomposition of unstable carbon on biochar surface [27]. After 25 dry-wet and freeze-thaw aging rounds, for Ca-SSBC, C contents decreased by 17.5% and 10.1%, respectively, while C contents in Ca-BDBC decreased by 25.8% and 14.6%, respectively (Figures 1b and 1d). It implied that exogenous Ca played a "protective" role on biochar, which defensed C loss. The O element contents increased remarkably along biochar aging. As shown in Figures S1a and S1c, O contents in SSBC increased by 18.2% and 10.1% after 25 dry-wet and freeze-thaw aging rounds, respectively, while that in BDBC increased by 18.9% and 6.28%, respectively. For Ca-SSBC, the O content increased by 33.6% and 19.1% after 25 dry-wet and freeze-thaw aging rounds, respectively, while that in Ca-BDBC increased by 27.3% and 6.86%, respectively (Figures S1b and S1d). Compared to pristine biochar, the addition of Ca could retain more O in biochar. XRD results confirmed that these O existed by the form of various minerals crystals, including CaO, $Ca_5(PO_4)Cl$, $Ca_5(PO_4)(OH)$, $Ca_8H_2(PO_4)_6{\cdot}H_2O$, and $Ca_{10}(PO_4)_6(OH)_2$ (Figure S2). These crystals could act as a "protective barrier" of biochar, and prevented C loss during aging. In addition, for H and N elements, their contents in pristine and Ca-rich biochar did not change regularly during aging, and fluctuated within a negligible range (Figures S1e-S1l). Only an obvious

Preprints (www.preprints.org) | NOT PEER-REVIEWED | Posted: 31 May 2023 doi:10.20944/preprints202305.2235.v1

decrease of N contents in aged BDBC and Ca-BDBC may be due to the volatilization of small N-containing components [28,29].

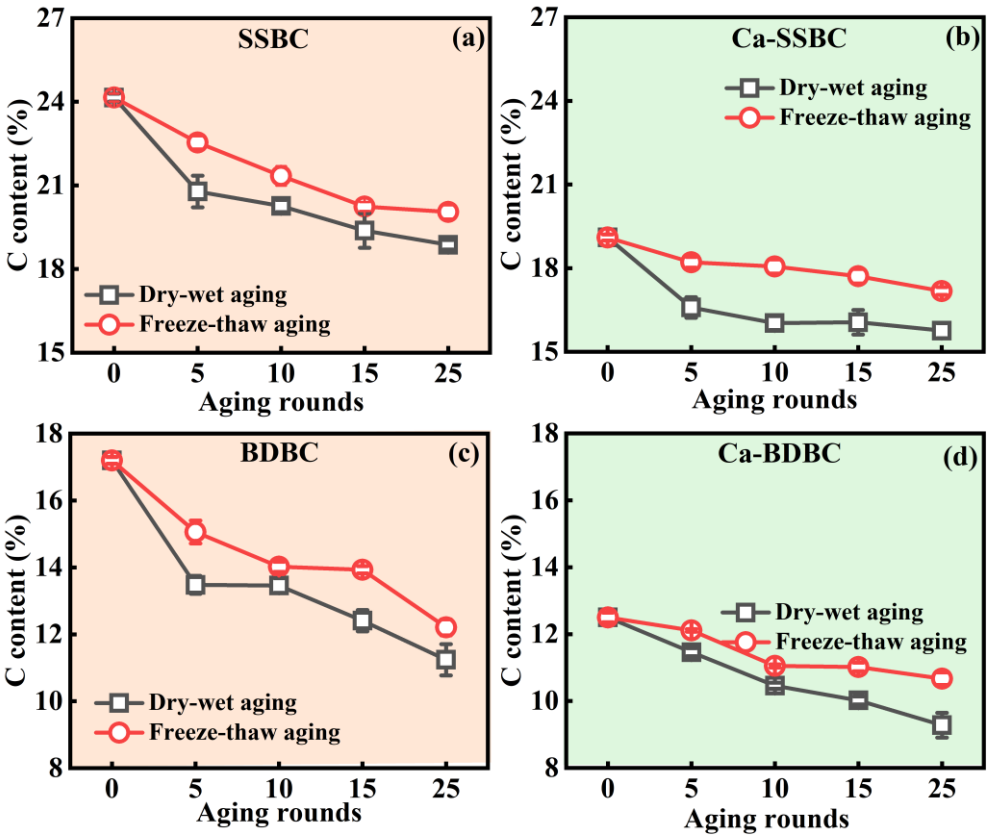

Figure 1. Variations of carbon (C) element contents in pristine biochar and Ca-rich biochar under different aging processes (n = 3) (SSBC: sewage sludge biochar; BDBC: bone dreg biochar; Ca-SSBC: $CaCl_2$ + sewage sludge biochar; Ca-BDBC: $CaCl_2$ + bone dreg biochar).

Changes of surface composition. The XPS results on the surface C bonding states for both pristine and Ca-rich biochar were shown in Figure S3. The C1s peaks were distinguished into four categories: aliphatic/aromatic peak (C–C/C = C) at 284.6 eV, ester peak (C–O) at 285.7 eV, carbonyl peak (C = O) at 287.0 eV, and carboxyl peak (O = C–O) at 288.7 eV [30–34]. Table 2 showed that 25 dry-wet (freeze-thaw) aging rounds caused the percentages of C–C/C = C (aliphatic/aromatic C) in SSBC and BDBC to decrease by 19% (14%) and 15% (12%), respectively. These lost aliphatic/aromatic C were transformed into O-containing functional groups [35], thus resulting in the obvious increase of C–O, C = O, and O = C–O. Shi et al. [31] also pointed out that the oxidative cleavage of some C–C bonds resulted in the formation of new C–O bonds during biochar aging. Similar to two pristine biochars, dry-wet and freeze-thaw aging treatments also resulted in more C–C/C = C in Ca-rich biochar to be transformed into C–O, C = O, and O = C–O. However, the decrements of C–C/C = C percentages in two pristine biochars were more than that in the corresponding Ca-rich biochar (Table 2), suggesting that the oxidation degree of C in the former was stronger than that in the later during aging.

Table 2. Content analysis of C bond states on biochar surface with different aging processes.

Biochar	Content/%	0 round	Dry-wet/25 rounds	Freeze-thaw/25 rounds
SSBC	C-C/C = C	79.20	64.51	67.74
	C = O	9.32	9.87	/
	O = C-O	7.19	5.28	10.58
	C-O	4.29	20.34	18.69

Preprints (www.preprints.org) | NOT PEER-REVIEWED | Posted: 31 May 2023 doi:10.20944/preprints202305.2235.v1

Ca-SSBC	C-C/C = C	74.79	65.06	68.60
	C = O	8.52	8.39	7.39
	O = C-O	8.42	6.29	7.96
	C-O	8.27	20.26	16.05
BDBC	C-C/C = C	67.75	57.47	59.85
	C = O	7.46	11.92	8.47
	O = C-O	8.69	11.97	9.70
	C-O	16.1	18.65	21.97
Ca-BDBC	C-C/C = C	65.18	60.01	62.64
	C = O	7.29	8.79	9.92
	O = C-O	14.48	10.40	5.82
	C-O	13.04	20.81	21.63

Changes of surface morphology. The SEM images of fresh and aged biochar samples were shown in Figure 2. The obvious and regular pore structure appeared in two pristine biochars, especially BDBC. After dry-wet or freeze-thaw aging, the surface smoothness of biochar decreased, and the regular pore structures began to collapse and disintegrate. Even some of resulting fragments began to block the pores of biochar. The results were consistent with previous studies [35,36]. The evolution of surface morphology of biochar during aging should attribute to two aspects. On the one hand, it was caused by physical disintegration of biochar structure [37]. Biochar would tend to fracture at relatively low strain under mechanical stress [38,39], while both dry-wet and freeze-thaw aging could provide sufficient conditions for the physical breakdown of biochar [40]. These two aging methods could cause the expansion and shrinkage of graphite sheets in biochar to occur alternately [39], ultimately resulting in the fragmentation of biochar structure. On the other hand, the chemical oxidation on biochar surface destroys its structure [30,31]. Unstable carbon on biochar surface could be oxidized by atmospheric oxygen, which introduced additional O-containing functional groups. Unlike the obvious pore structure in pristine biochar, the smooth coating covered on the surface of Ca-rich biochar (Figure 2). After 25 dry-wet or freeze-thaw aging rounds, a crevice structure appeared on Ca-rich biochar surface. The new structure was like a "web" with several broken holes, which served as a physical barrier to inhibit the oxidation of carbon during Ca-rich biochar aging [19,41,42].

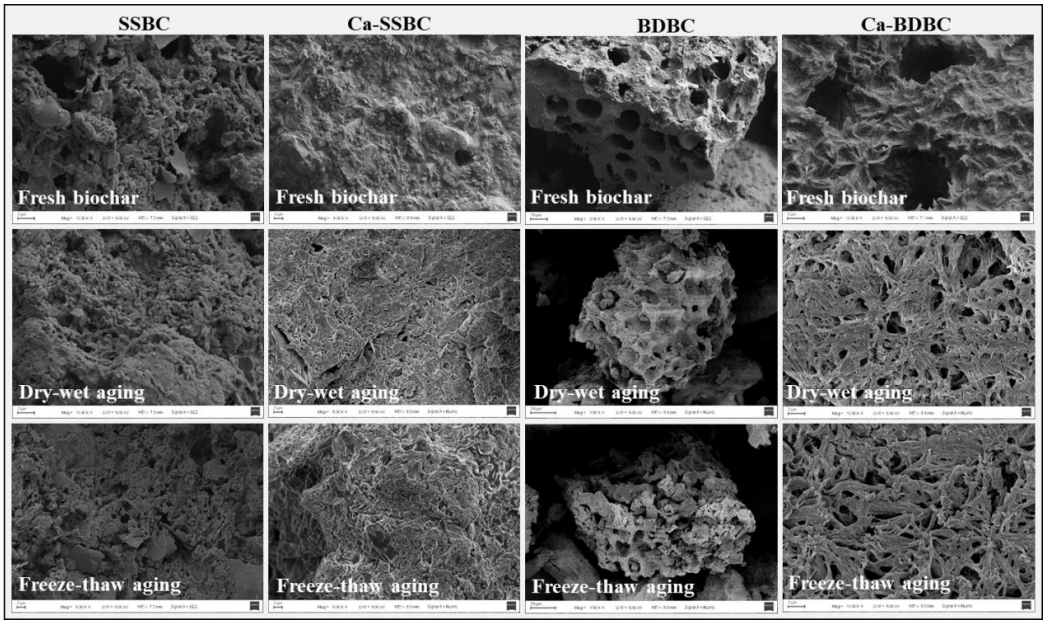

Figure 2. Morphology changes of pristine biochar (SSBC: sewage sludge biochar; BDBC: bone dreg biochar) and Ca-rich biochar (Ca-SSBC: $CaCl_2$+sewage sludge biochar; Ca-BDBC: $CaCl_2$+bone dreg biochar) under different aging processes.

Preprints (www.preprints.org) | NOT PEER-REVIEWED | Posted: 31 May 2023 doi:10.20944/preprints202305.2235.v1

3.2. Exogenous calcium enhanced the surface C stability in biochar during aging process

Dry-wet aging. Based on the eq. 1 (Section 2.2), this study quantified the surface C stability in pristine biochar and Ca-rich biochar during dry-wet aging. As shown in Figures 3a and 3b, with the increase of aging round, the oxidized surface C in both pristine biochar and Ca-rich biochar increased obviously. In this study, the oxidized surface C in fresh biochar was defined as zero. After 25 dry-wet aging rounds, its contents in SSBC and BDBC increased to 22% and 35%, respectively, while that in Ca-SSBC and Ca-BDBC decreased by 20% and 10% than that in SSBC and BDBC, respectively. Dry-wet aging induced the oxidation of surface C by causing the destruction of C structure in biochar [31]. Usually, dry-wet aging of biochar was accompanied by the absorption–drying–reabsorption process of water on its surface, which could change the sag diameter, crack size and pore structure of biochar particles, and eventually led to the collapse of biochar structures and the generation of more liberated biochar fragments [39]. These biochar fragments, as fresh exposures, were prone to occur surface mineralization or abiotic oxidization [43,44]. As shown in Figure 2, dry-wet aging resulted in the surface of SSBC and BDBC to become rough, and pore structures began to collapse and disintegrate. Meanwhile, dry-wet aging could destroy biochar' composition by chemical reactions. The XPS results showed that the percentages of C = O, O = C–O, and C–O in fresh biochar were lower than that in aged biochar (Figure S3 and Table 2), suggesting that aging resulted in the oxidization of biochar [25]. By contrasting C bond states of pristine biochar and Ca-rich biochar after dry-wet aging (Table 2), the percentages of C = O, O = C–O, and C–O in the former was more than that in the latter, which was corresponding with their surface C stability (Figures 3a and 3b). This phenomenon should attribute to the "protective effect" of abundant Ca-containing crystals to the surface C in Ca-rich biochar (Figure S2). These crystals acted as a surface "armor" of Ca-rich biochar to prevent external oxygen from contacting with biochar, thus inhibiting the oxidation of surface C. Additionally, the crevice structures like "web" appearing on the surface of Ca-SSBC and Ca-BDBC were very likely to serve as a physical barrier to inhibit the oxidization of surface C in biochar (Figure 2).

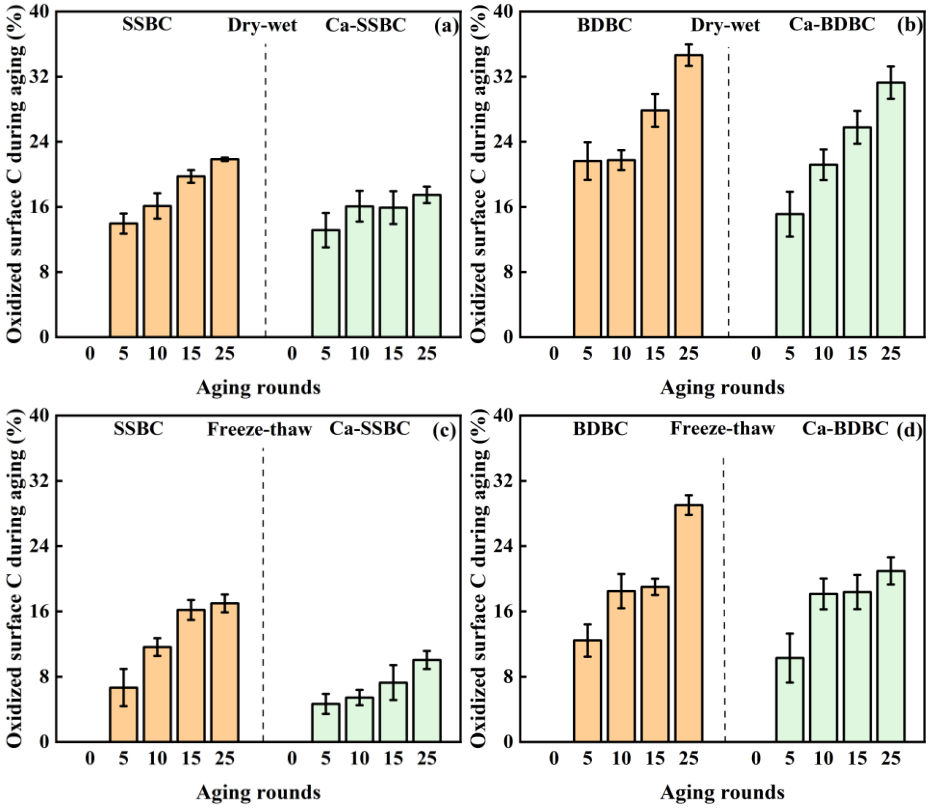

Preprints (www.preprints.org) | NOT PEER-REVIEWED | Posted: 31 May 2023 doi:10.20944/preprints202305.2235.v1

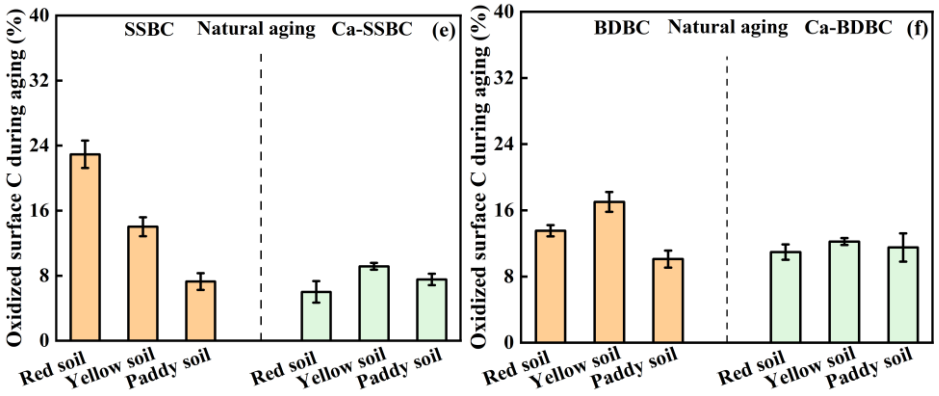

Figure 3. Variation of surface C stability in pristine biochar (SSBC: sewage sludge biochar; BDBC: bone dreg biochar) and Ca-rich biochar (Ca-SSBC: $CaCl_2$ + sewage sludge biochar; Ca-BDBC: $CaCl_2$ + bone dreg biochar) during different aging processes (n = 3).

Freeze-thaw aging. Similar to dry-wet aging, the oxidized surface C in pristine biochar and Ca-rich biochar also increased with the increase of freeze-thaw aging rounds. As shown in Figures 3c and 3d, after 25 freeze-thaw aging rounds, the percentages of oxidized C in SSBC and BDBC were increased from zero to 17% and 29%, respectively, while that in Ca-SSBC and Ca-BDBC increased from zero to 10% and 21%, respectively. Obviously, the oxidized surface C contents in biochar caused by freeze-thaw aging was lower than that caused by dry-wet aging (Figures 3a–3d). This was due to the difference in the destruction mode and degree of carbon structure caused by the two aging processes. The freeze-thaw aging of biochar was usually accompanied by the expansion–shrinkage–re-expansion process of water in its interior [37,40]. Freezing treatment caused the expansion and embrittlement of biochar structure and the intergranular and intragranular extrusion of biochar, resulting the deformation and fragmentation of biochar structure [45]. The subsequent thaw treatment resulted in the penetration of water into biochar interior along surface pore or capillary pathways, further rearranging and translocating the biochar fragments [46,47]. Compared with the dry cracking of biochar structure caused by high temperature, the brittle cracking caused by low temperature has more mild damage to C structure in biochar [36]. The XPS results from Table 2 also confirmed this phenomenon and displayed that the contents of C = O, O = C–O, and C–O in aged biochar with the freeze-thaw treatment were less than that with the dry-wet treatment. Meanwhile, after 25 freeze-thaw aging rounds, the contents of C = O, O = C–O, and C–O in pristine biochar were more than in the corresponding Ca-rich biochar, suggesting that mineral Ca in Ca-rich biochar also inhibited the oxidization of surface C in biochar during freeze-thaw aging. Like the dry-wet aging, obvious "net" structure was also found on Ca-rich biochar surface after freeze-thaw aging (Figure 2). Therefore, during freeze-thaw aging, the protective effect of mineral Ca on Ca-rich biochar surface was still the dominant factor to enhance the surface C stability in biochar.

Natural aging in farmland soil. Unlike the dry-wet and freeze-thaw aging, applying biochar in soil could create the realistic aging scenario, which was of more practical value for measuring the surface C stability in biochar. As shown in Figures 3e and 3f, the pristine biochar and Ca-rich biochar lost 7~23% C and 6~12% C after undergoing five-month natural aging in three farmland soils, respectively. The C loss should be attributed to three aspects. Firstly, the unstable C on biochar surface was oxidized by soil components and atmospheric oxygen in the early stage of applying biochar in soil [48,49]. Secondly, biochar released some soluble organic components in soil and participated in the complex redox processes [27,29], resulting the oxidation of C. Thirdly, the soil environment accelerated the fragmentation of biochar, resulting in the exposure of its active surface and further oxidation [38,39]. While it was worth noting that the oxidized surface C from two pristine biochars in three soils were obviously more than that of corresponding Ca-rich biochar (Figures 3e and 3f). Taking red soil for example, the oxidized surface C in SSBC and BDBC

 doi:10.20944/preprints202305.2235.v1

were 23% and 14%, respectively, while in corresponding Ca-rich biochar, they decreased to 6% and 11%, respectively. The similar results also appeared in yellow soil and paddy soil. Obviously, considering the surface C stability of biochar in soil, Ca-rich biochar was more dominant than pristine biochar. It was inseparable from the action of Ca-containing mineral crystals on the Ca-rich biochar surface (Figure S2), which could isolate biochar with the oxygen, soil microbes, and active enzymes from the soil environment and slow down the oxidization of surface C in biochar during mineralization [50]. Even, mineral Ca on Ca-rich biochar surface could serve as the "bridge" to connect clay mineral particles in soil and organic C in biochar [50], which reinforced the "protective barrier" of biochar, thus resisting degradation of C in biochar [51].

3.3. Exogenous calcium enhanced the bulk C stability in biochar during aging process

Dry-wet aging. The $K_2Cr_2O_7$ oxidization treatment of biochar is an important method to assess the bulk C stability [52]. As shown in Figures 4a and 4b, for SSBC and BDBC, after 25 dry-wet aging rounds, the oxidized C contents increased from 26% to 49% and from 40% to 65%, respectively. It should attribute to that dry-wet aging caused the formation of more biochar fragments (Figure 2), which were prone to be oxidized and broken down [43,44]. Furthermore, dry-wet aging resulted in more aliphatic/aromatic C to be oxidized (Table 2), which destroyed the order and regularity of the carbon structure, thus exposing more unstable C [37,53]. The oxidized C contents in two fresh Ca-rich biochar samples were higher than that in corresponding pristine biochar. As shown in Figures 4c and 4d, the percentages of oxidized C in fresh SSBC, Ca-SSBC, BDBC, and Ca-BDBC were 25.7%, 28.6%, 39.4%, and 46.1%, respectively. In our previous study, we attributed this phenomenon to that mineral Ca induced the formation of more disordered carbon structures during biowaste pyrolysis [19]. Similar to pristine biochar, the oxidized bulk C contents in Ca-rich biochar increased with the increase of aging rounds (Figures 4c and 4d). After 25 dry-wet aging rounds, the contents of oxidized bulk C in Ca-SSBC and Ca-BDBC increased to 44% and 61%, respectively, and they were less than that in corresponding pristine biochar. Here we focused on an interesting phenomenon that after 25 dry-wet aging rounds, the rates of increase about the oxidized bulk C from SSBC and BDBC were 89% and 65%, respectively, and that from Ca-SSBC and Ca-BDBC were 55% and 32%, respectively. The rates of increase about the oxidized C from two Ca-rich biochars were obviously lower than that from corresponding pristine biochar. It indicated that the effect of dry-wet aging on bulk C stability in Ca-rich biochar was weaker than that in pristine biochar. This was due to the protective layer formed by mineral Ca on biochar surface, which could alleviate the damage of the biochar surface structure during the aging process [47,54–56]. The conjecture could be verified by XPS results (Figure S2 and Table 2). The percentages of C–C/C = C in pristine biochar decreased by 19% (SSBC) and 15% (BDBC) after 25 rounds dry-wet aging, respectively, while that in Ca-rich biochar decreased by 13% (Ca-SSBC), and 8% (Ca-BDBC), respectively. Combining with SEM in Figure 2 and XRD in Figure S2, it was confirmed mineral Ca could provide a physical isolation to prevent the contact of carbon in biochar and external O_2, thus reducing formation of O-containing functional groups on biochar surface [47]. Therefore, compared with the pristine biochar, it was more difficult to destroy bulk C structure in Ca-rich biochar during dry-wet aging. Figure 5 further showed that O/C ratio was positively correlated with the content of oxidized bulk C in both pristine biochar and Ca-rich biochar, indicating that the surface oxidation degree of biochar directly affected the bulk C stability [57,58].

Preprints (www.preprints.org) | NOT PEER-REVIEWED | Posted: 31 May 2023 doi:10.20944/preprints202305.2235.v1

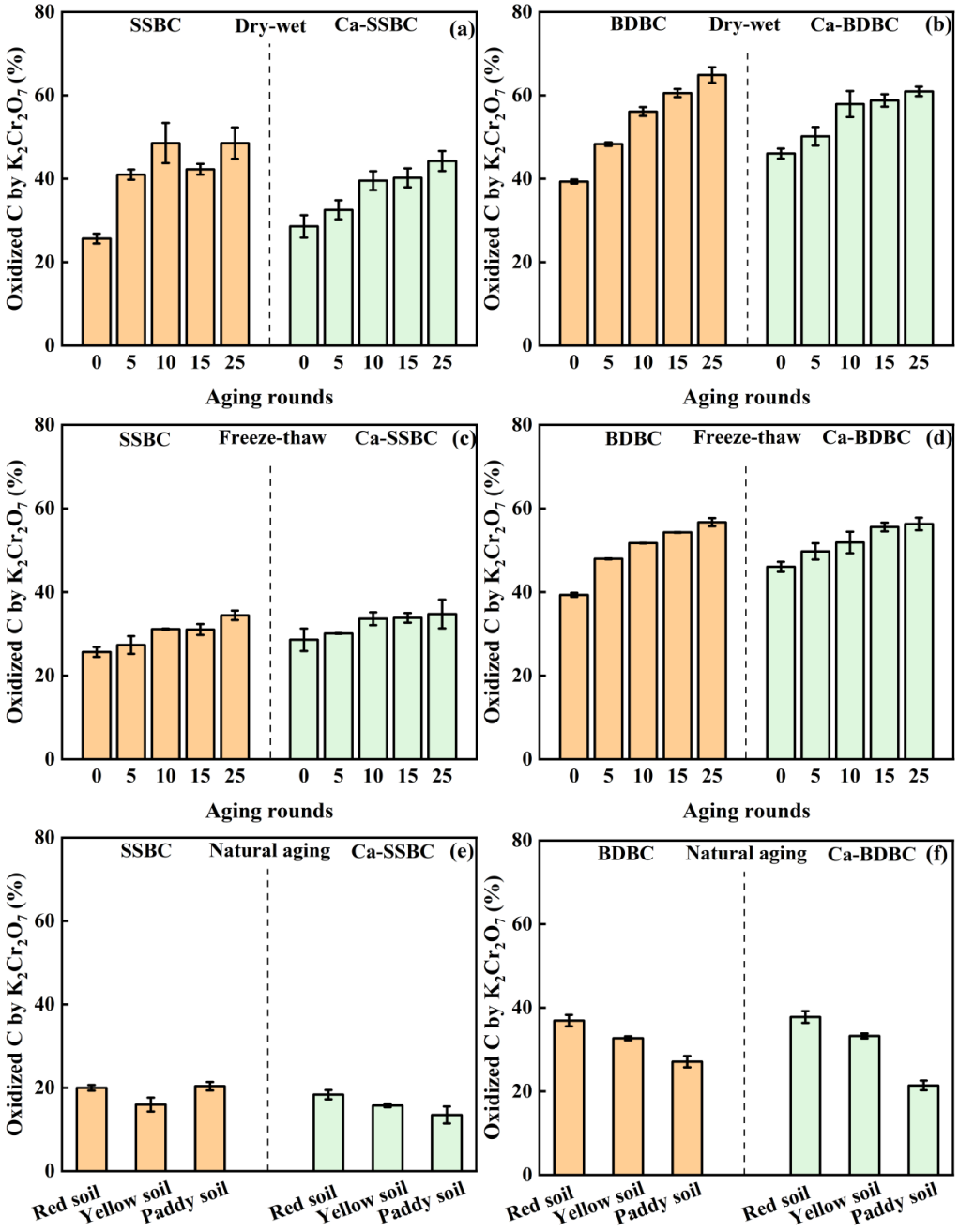

Figure 4. Variation of bulk C stability in pristine biochar (SSBC: sewage sludge biochar; BDBC: bone dreg biochar) and Ca-rich biochar (Ca-SSBC: $CaCl_2$+sewage sludge biochar; Ca-BDBC: $CaCl_2$+bone dreg biochar) during different aging processes (n = 3).

Preprints (www.preprints.org) | NOT PEER-REVIEWED | Posted: 31 May 2023 doi:10.20944/preprints202305.2235.v1

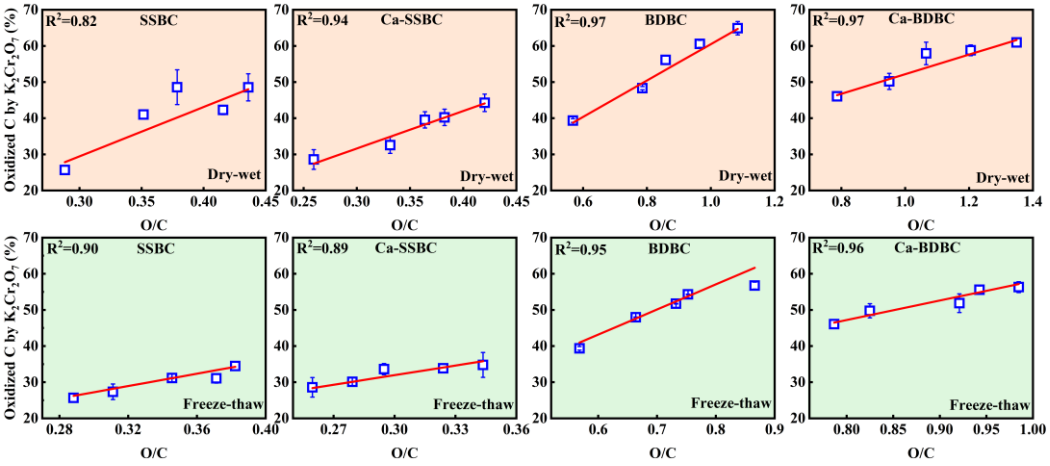

Figure 5. Relationship between O/C atom ratio and oxidized C by $K_2Cr_2O_7$ in pristine biochar (SSBC: sewage sludge biochar; BDBC: bone dreg biochar) and Ca-rich biochar (Ca-SSBC: $CaCl_2$ + sewage sludge biochar; Ca-BDBC: $CaCl_2$ + bone dreg biochar) during different aging processes (n = 3).

Freeze-thaw aging. Freeze-thaw aging also decreased bulk C stability in biochar (Figures 4c and 4d). For SSBC and BDBC, after 25 rounds freeze-thaw aging, the contents of oxidized bulk C increased from 26% to 34% and from 39% to 57%, respectively, while that in Ca-SSBC and Ca-BDBC increased from 29% to 35% and from 46% to 56%, respectively. It was unexpected that after 25 freeze-thaw aging rounds, the oxidized bulk C contents in two Ca-rich biochars were almost uniform with that from two pristine biochars, while the rates of increase about the oxidized bulk C decreased from 34% (SSBC) to 22% (Ca-SSBC) and from 44% (BDBC) to 22% (Ca-BDBC), respectively. XPS results showed that compared to fresh biochar, the freeze-thaw aging resulted in the percentages of C = O, O = C-O, and C-O in SSBC and BDBC to increase by 55% and 24%, respectively, and that in Ca-SSBC and Ca-BDBC to increase by 25% and 7%, respectively (Table 2), indicating that Ca-rich biochar had stronger antioxidative capacity than pristine biochar. Meanwhile, unlike the fragment structure of pristine biochar after freeze-thaw aging, the SEM images of Ca-rich biochar presented the obvious "net" pore structure (Figure 2), which intervened the oxidization of bulk C in biochar.

Natural aging in soil. After natural aging, biochar was isolated from soil and its bulk C stability was evaluated by $K_2Cr_2O_7$ oxidized method. As shown in Figure 4e, after natural aging in red soil, yellow soil, and paddy soil for five months, oxidized bulk C contents in SSBC were 20%, 16%, and 20%, respectively, while that in BDBC were 37%, 33%, and 27%, respectively. They were lower than the corresponding fresh biochar (26% in SSBC and 39% in BDBC). This phenomenon was closely related to soil components, mainly soil minerals. On the one hand, the adsorption of soil minerals onto biochar could serve as the physical barrier and prevent its decomposition and oxidation processes [55,56]. On the other hand, the interaction of biochar with soil minerals induced the formation of biochar–mineral complexes [47], which inhibited the oxidation of biochar the by occupying its surface reaction site or blocking its pores [54]. After natural aging in different soils, oxidized bulk C contents in Ca-rich biochar were obviously lower than that in pristine biochar (Figure 4f). Oxidized bulk C contents in Ca-SSBC were 18% (red soil), 16% (yellow soil), and 13% (paddy soil), respectively, which were decreased by 8%, 1%, and 34% than that in SSBC, respectively. For Ca-BDBC with natural aging in red soil and yellow soil, the oxidized C contents were nearly equal to that in BDBC, while in paddy soil, the oxidized C contents in Ca-BDBC decreased by 21% than that in BDBC. Therefore, from the perspective of long-term stability of biochar in soil, Ca-rich biochar was more suitable than pristine biochar.

3.4. Exogenous calcium enhanced C sequestration ability in biochar during aging process

Preprints (www.preprints.org) | NOT PEER-REVIEWED | Posted: 31 May 2023 doi:10.20944/preprints202305.2235.v1

In this study, the initial carbon content of all fresh biochar was normalized to 100%, and the carbon sequestration in biochar during aging was roughly estimated by considering both surface C stability and bulk C stability. After 25 dry-wet aging rounds, for SSBC and BDBC, the final C sequestration contents were decreased from 74% to 40% and from 61% to 23%, respectively (Figures 6a and 6b). While C contents sequestrated in Ca-rich biochar were 46% (Ca-SSBC) and 27% (Ca-BDBC), respectively. After 25 freeze-thaw aging rounds, the final C sequestration contents in SSBC and BDBC were decreased to 55% and 31%, respectively, while the C contents sequestrated in Ca-rich biochar were 59% (Ca-SSBC) and 35% (Ca-BDBC), respectively (Figures 6c and 6d). The results indicated that when the initial carbon content kept equal, two Ca-rich biochars could sequestrate more carbon than the corresponding pristine biochar under dry-wet or freeze-thaw aging. In addition, it was worth noting that the influence of freeze-thaw aging on C stability was weaker than that of dry-wet aging, suggesting that biochar was more suitable to be applied in the northern permafrost than in the southern dry soil. After natural aging in three farmland soils for five months, the final C sequestration contents in SSBC were 62% (red soil), 72% (yellow soil), and 74% (paddy soil), respectively (Figure 6e). For Ca-SSBC, their contents were 77% (red soil), 77% (yellow soil), and 80% (paddy soil), respectively, indicating that Ca-SSBC was more stable in soil than SSBC. The similar results also appeared in BDBC and Ca-BDBC (Figure 6f). In all, Ca-rich biochar could sequestrate more C than pristine biochar under all three aging processes. Therefore, it will own greater application potential than pristine biochar.

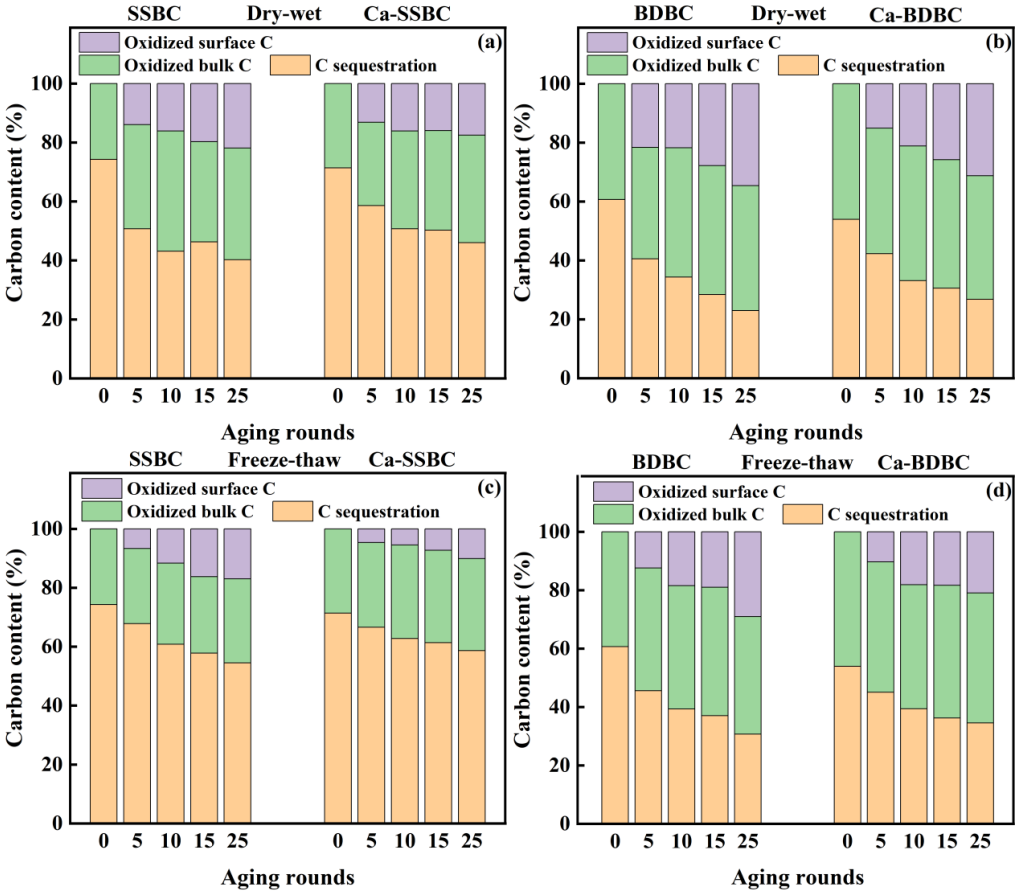

Preprints (www.preprints.org) | NOT PEER-REVIEWED | Posted: 31 May 2023 doi:10.20944/preprints202305.2235.v1

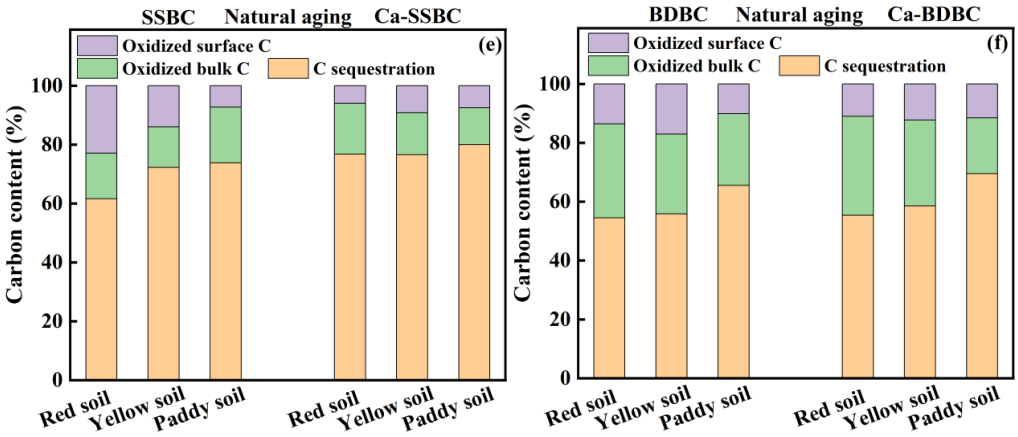

Figure 6. Carbon content sequestrated in pristine biochar (SSBC: sewage sludge biochar; BDBC: bone dreg biochar) and Ca-rich biochar (Ca-SSBC: $CaCl_2$ + sewage sludge biochar; Ca-BDBC: $CaCl_2$ + bone dreg biochar) during different aging processes.

4. Conclusions

In this study, exogenous calcium is used to enhance biochar stability without increasing pyrolysis temperature and consuming more energy, which is not only easy to operate and low-cost, but also convenient for large-scale popularization and application. It is of great significance for realizing carbon sequestration by biochar. This study found that under three aging processes (dry-wet aging, freeze-thaw aging, and natural aging), both surface C and bulk C stability of two Ca-rich biochars were superior to that of corresponding pristine biochar. It was attributed to that exogenous Ca on Ca-SSBC and Ca-BDBC surface acted as a "physical barrier", which blocked the connection between biochar-C and external oxidizing environment, and intervened the oxidation of C-C/C = C. Additionally, the "physical barrier" protected C skeleton structure of biochar, reducing the generation of fragmented structure. Eventually, with the addition of exogenous Ca, the maximal C sequestration in SSBC and BDBC increased by 24.4% and 16.9% under three aging processes, respectively. It implies that when using biochar for carbon sequestration, exogenous calcium can be added to the precursors to enhance the stability of biochar and improve carbon sequestration efficiency.

Supplementary Materials: The following supporting information can be downloaded at: www.mdpi.com/xxx/s1, Table S1: Main element contents and pore structure parameters of four biochars. Figure S1: Variations of oxygen (O), hydrogen (H), and nitrogen (N) element contents in pristine biochar and Ca-rich biochar under different aging processes. Figure S2: Surface crystals compositions of pristine biochar. Figure S3: Surface carbon functional groups of pristine biochar and Ca-rich biochar with different aging processes.

Author Contributions: H.N.: Conceptualization; Methodology; Investigation; Data curation; Formal analysis; Writing—original draft. Y.J.: Methodology; Formal analysis; Writing—Reviewing and Editing. W.Z.: Formal analysis; Writing—Reviewing and Editing. L.Z.: Supervision; Writing—Reviewing and Editing. F.Y.: Supervision; Funding acquisition; Conceptualization; Writing—Reviewing and Editing. All authors have read and agreed to the published version of the manuscript.

Funding: This work is supported by Science and Technology Commission of Shanghai Municipality (No.22dz1209402); Study on low concentration urban biological nitrogen removal technology based on autotrophic denitrification of sulfur and iron.

Conflicts of Interest: The authors declare no conflict of interest.

References

1. Cheng, C.H., Lehmann, J., Engelhard, M.H., 2008. Natural oxidation of black carbon in soils: Changes in molecular form and surface charge along a climosequence. Geochim. Cosmochim. Ac. 72(6), 1598-1610.
2. Lehmann, J., 2007. A handful of carbon. Nature 447(7141), 143-144.

3. Lehmann, J., Skjemstad, J., Sohi, S., Carter, J., Barson, M., Falloon, P., Coleman, K., Woodbury, P., Krull, E., 2008. Australian climate–carbon cycle feedback reduced by soil black carbon. Nat. Geosci. 1(12), 832-835.
4. Spokas, Kurt, A., 2010. Review of the stability of biochar in soils: predictability of O:C molar ratios. Carbon Manage. 1(2), 289-303.
5. Woolf, D., Amonette, J.E., Street-Perrott, F.A., Lehmann, J., Joseph, S., 2010. Sustainable biochar to mitigate global climate change. Nat. Commun. 1(1), 56.
6. Sohi, S.P., Krull, E., Lopez-Capel, E., Bol, R., 2010. A review of biochar and its use and function in soil. Adv. Agron. 105, 47-82.
7. Hammes, K., Torn, M.S., Lapenas, A.G., Schmidt, M.W.I., 2008. Centennial black carbon turnover observed in a Russian steppe soil. Biogeosciences 5, 1339-1350.
8. Masek, O., Brownsort, P., Cross, A., Sohi, S., 2013. Influence of production conditions on the yield and environmental stability of biochar. Fuel 103, 151-155.
9. Singh, B.P., Cowie, A.L., Smernik, R.J., 2012. Biochar carbon stability in a clayey soil as a function of feedstock and pyrolysis temperature. Environ. Sci. Technol. 46(21), 11770.
10. Mcbeath, A.V., Wurster, C.M., Bird, M.I., 2015. Influence of feedstock properties and pyrolysis conditions on biochar carbon stability as determined by hydrogen pyrolysis. Biomass Bioenerg. 73, 155-173.
11. Purakayastha, T.J., Kumari, S., Pathak, H., 2015. Characterisation, stability, and microbial effects of four biochars produced from crop residues. Geoderma 239-240, 293-303.
12. Fang, Y., Singh, B., Singh, B.P., 2015. Effect of temperature on biochar priming effects and its stability in soils. Soil Bio. Biochem. 80(80), 136-145.
13. Han, L., Ro, K.S., Wang, Y., Sun, K., Sun, H., Libra, J.A., Xing, B., 2018. Oxidation resistance of biochars as a function of feedstock and pyrolysis condition. Sci. Total Environ. 616-617, 335-344.
14. Liu, Y., Yao, S., Wang, Y., Haohao, L., Brar, S.K., Yang, S., 2017. Bio- and hydrochars from rice straw and pig manure: Inter-comparison. Bioresource Technol. 235, 332-337.
15. Leng, L., Huang, H., 2018. An overview of the effect of pyrolysis process parameters on biochar stability. Bioresource Technol. 270, 627-642.
16. Xu, X., Hu, X., Ding, Z., Chen, Y., 2017. Effects of copyrolysis of sludge with calcium carbonate and calcium hydrogen phosphate on chemical stability of carbon and release of toxic elements in the resultant biochars. Chemosphere 189, 76-85.
17. Du, J., Zhang, L., Ali, A., Li, R., Xiao, R., Guo, D., Liu, X., Zhang, Z., Ren, C., Zhang, Z., 2019. Research on thermal disposal of phytoremediation plant waste: Stability of potentially toxic metals (PTMs) and oxidation resistance of biochars. Process Saf. Environ. 125, 260-268.
18. Chen, D., Yu, X., Song, C., Pang, X., Huang, J., Li, Y., 2016. Effect of pyrolysis temperature on the chemical oxidation stability of bamboo biochar. Bioresource Technol. 218, 1303-1306.
19. Nan, H., Zhao, L., Yang, F., Liu, Y., Qiu, H., 2020. Different alkaline minerals interacted with biomass carbon during pyrolysis: Which one improved biochar carbon sequestration? J. Clean. Prod. 255, 120162.
20. Wu, X., Radovic, L.R., 2006. Inhibition of catalytic oxidation of carbon/carbon composites by phosphorus. Carbon 44(1), 141-151.
21. Rosas, J.M., Ruiz-Rosas, R., Rodríguez-Mirasol, J., Cordero, T., 2012. Kinetic study of the oxidation resistance of phosphorus-containing activated carbons. Carbon 50(4), 1523-1537.
22. Guo, J., Chen, B., 2014. Insights on the molecular mechanism for the recalcitrance of biochars: interactive effects of carbon and silicon components. Environ. Sci. Technol. 48(16), 9103-9112.
23. Xin, X., Chen, B., Zhu, L., 2014. Transformation, morphology, and dissolution of silicon and carbon in rice straw-derived biochars under different pyrolytic temperatures. Environ. Sci. Technol. 48(6), 3411-3419.
24. Lu, J., Yang, Y., Liu, P., Li, Y., Huang, F., Zeng, L., Liang, Y., Li, S., Hou, B., 2020. Iron-montmorillonite treated corn straw biochar: Interfacial chemical behavior and stability Sci. Total Environ. 708, 134773.
25. Hale, S., Hanley, K., Lehmann, J., Zimmerman, R., Cornelissen, G., 2011. Effects of chemical, biological, and physical aging as well as soil addition on the sorption of pyrene to activated carbon and biochar. Environ. Sci. Technol. 45(24), 10445-10453.
26. Zhang, P., Fan, J., Xu, X., Xu, Z., Yu, Y., Zhao, L., Qiu, H., Cao, X., 2022. Contrasting effects of dry-wet and freeze-thaw aging on the immobilization of As in As-contaminated soils amended by zero-valent iron-embedded biochar. J. Hazard. Mater. 426, 128123.
27. Andrew, R.Z., 2010. Abiotic and microbial oxidation of laboratory-produced black carbon (biochar). Environ. Sci. Technol. 44(4), 1295-1301.
28. Liu, D., Liu, D., Gao, J., Yang, Y., Ding, Y., Guo, C., Zhang, X., Xia, Z., Xu, W., 2022. Influence of addition of two typical activated carbons on fertility properties and mechanical strength of vegetation concrete under freeze-thaw conditions. Sci. Total Environ. 838, 156446.
29. Mukherjee, A., Zimmerman, A.R., 2013. Organic carbon and nutrient release from a range of laboratory-produced biochars and biochar–soil mixtures. Geoderma 193-194, 122-130.
30. Fan, Q., Sun, J., Chu, L., Cui, L., Quan, G., Yan, J., Hussain, Q., Iqbal, M., 2018. Effects of chemical oxidation on surface oxygen-containing functional groups and adsorption behavior of biochar. Chemosphere 207, 33-40.
31. Shi, K., Xie, Y., Qiu, Y., 2015. Natural oxidation of a temperature series of biochars: opposite effect on the sorption of aromatic cationic herbicides. Ecotox. Environ. Safe. 114, 102-108.

 doi:10.20944/preprints202305.2235.v1

32. Singh, B., Fang, Y., Cowie, B., Thomsen, L., 2014. NEXAFS and XPS characterisation of carbon functional groups of fresh and aged biochars. Org. Geochem. 77, 1-10.
33. Yao, F.X., Arbestain, M.C., Virgel, S., Blanco, F., Arostegui, J., Maciá-Agulló, J.A., Macías, F., 2010. Simulated geochemical weathering of a mineral ash-rich biochar in a modified Soxhlet reactor. Chemosphere 80(7), 724-732.
34. Fang, Q., Chen, B., Lin, Y., Guan, Y., 2014. Aromatic and hydrophobic surfaces of wood-derived biochar enhance perchlorate adsorption via hydrogen bonding to oxygen-containing organic groups. Environ. Sci. Technol. 48, 279-288.
35. Ren, X., Sun, H., Wang, F., Zhang, P., Zhu, H., 2018. Effect of aging in field soil on biochar's properties and its sorption capacity. Environ. Pollut. 242, 1880-1886.
36. Cao, Y., Jing, Y., Hao, H., Wang, X., 2019. Changes in the physicochemical characteristics of peanut straw biochar after freeze-thaw and dry-wet aging treatments of the biomass. Bioresources 14(2), 4329-4343.
37. Wang, L.W., O'Connor, D., Rinklebe, J., Ok, Y.S., Tsang, D.C.W., Shen, Z.T., Hou, D.Y., 2020. Biochar aging: mechanisms, physicochemical changes, assessment, and implications for field applications. Environ. Sci. Technol. 54(23), 14797-14814.
38. Gao, X., Wu, H., 2013. Aerodynamic properties of biochar particles: effect of grinding and implications. Environ. Sci. Technol. Let. 1(1), 60-64.
39. Spokas, K.A., Novak, J.M., Masiello, C.A., Johnson, M.G., Colosky, E.C., Ippolito, J.A., Trigo, C., 2014. Physical disintegration of biochar: an overlooked process. Environ. Sci. Technol. Let. 1(8), 326-332.
40. Tan, L., Ma, Z., Yang, K., Cui, Q., Zheng, J., 2019. Effect of three artificial aging techniques on physicochemical properties and Pb adsorption capacities of different biochars. Sci. Total Environ. 699, 134223.
41. Rosas, J.M., Ruiz-Rosas, R., Rodríguez-Mirasol, J., Cordero, T., 2012. Kinetic study of the oxidation resistance of phosphorus-containing activated carbons. Carbon 50(4), 1523-1537.
42. Nan, H., Mašek, O., Yang, F., Xu, X., Qiu, H., Cao, X., Zhao, L., 2022. Minerals: A missing role for enhanced biochar carbon sequestration from the thermal conversion of biomass to the application in soil. Earth-Sci. Rev. 234, 104215.
43. Sigua, G.C., Novak, J.M., Watts, D.W., Cantrell, K.B., Shumaker, P.D., Szoegi, A.A., Johnson, M.G., 2014. Carbon mineralization in two ultisols amended with different sources and particle sizes of pyrolyzed biochar. Chemosphere 103, 313-321.
44. Huisman, D.J., Braadbaart, F., Wijk, I., Os, B., 2012. Ashes to ashes, charcoal to dust: micromorphological evidence for ash-induced disintegration of charcoal in Early Neolithic (LBK) soil features in Elsloo (The Netherlands). J. Archaeol. Sci. 39(4), 994-1004.
45. Liu, W., Wang, Y., Chen, D., Lu, P., 2021. Effect of aging on physicochemical properties of bio-chars. J. Eng. Thermophy. 42(6), 1575-1582.
46. Hillel, D., 2003. Introduction to Environmental Soil Physics: Chapter 1- Soil Physics and Soil Physical Characteristics. Academic Press (Eds.1), 3-17.
47. Yang, F., Zhao, L., Gao, B., Xu, X., Cao, X., 2016. The interfacial behavior between biochar and soil minerals and its effect on biochar stability. Environ. Sci. Technol. 2264-2271.
48. Li, H., Lu, X., Xu, Y., Liu, H., 2019. How close is artificial biochar aging to natural biochar aging in fields? A meta-analysis. Geoderma 352, 96-103.
49. Wang, H., Feng, M., Zhou, F., Huang, X., Tsang, D., Zhang, W., 2017. Effects of atmospheric ageing under different temperatures on surface properties of sludge-derived biochar and metal/metalloid stabilization. Chemosphere 184, 176.
50. Yang, F., Xu, Z.B., Lu, Y., Gao, B., Xu, X., Zhao, L., Cao, X., 2018. Kaolinite enhances the stability of the dissolvable and undissolvable fractions of biochar via different mechanisms. Environ. Sci. Technol. 52(15), 8321-8329.
51. Skjemstad, J.O., Clarke, P., Taylor, J.A., Oades, J.M., Mcclure, S.G., 1996. The chemistry and nature of protected carbon in soil. Soil Res. 34(2), 1876-1880.
52. Li, F., Cao, X., Zhao, L., Wang, J., Ding, Z., 2014. Effects of mineral additives on biochar formation: Carbon retention, stability, and properties. Environ. Sci. Technol. 48(19), 11211-7.
53. Mia, S., Dijkstra, F.A., Singh, B., 2017. Long-term aging of biochar: a molecular understanding with agricultural and environmental implications. Adv. Agron. 141, 1-51.
54. Ren, X., Wang, F., Zhang, P., Guo, J., Sun, H., 2018b. Aging effect of minerals on biochar properties and sorption capacities for atrazine and phenanthrene. Chemosphere 206, 51-58.
55. Nguyen, B.T., Lehmann, J., Kinyangi, J., Smernik, R., Riha, S.J., Engelhard, M.H., 2009. Long-term black carbon dynamics in cultivated soil. Biogeochemistry 92(1), 163-176.
56. Lin, Y., Munroe, P., Joseph, S., Kimber, S., Zwieten, L.V., 2012. Nanoscale organo-mineral reactions of biochars in ferrosol: an investigation using microscopy. Plant Soil 357(1), 369-380.
57. Crombie, K., Mašek, O., Sohi, S.P., Brownsort, P., Cross, A., 2013. The effect of pyrolysis conditions on biochar stability as determined by three methods. GCB Bioenergy 5(2), 122-131.
58. Andrew, C., Saran, P.S., 2013. A method for screening the relative long-term stability of biochar. GCB Bioenergy 5(2), 215-220.